

# UC Merced

## UC Merced Previously Published Works

### Title

Unveiling the cold reality of metamorphic proteins.

### Permalink

<https://escholarship.org/uc/item/7q61308q>

### Journal

Proceedings of the National Academy of Sciences of the United States of America,  
122(12)

### ISSN

0027-8424

### Authors

LiWang, Andy  
Orban, John

### Publication Date

2025-03-25

### DOI

10.1073/pnas.2422725122

### Copyright Information

This work is made available under the terms of a Creative Commons Attribution-NonCommercial-NoDerivatives License, available at  
<https://creativecommons.org/licenses/by-nc-nd/4.0/>

Peer reviewed



# Unveiling the cold reality of metamorphic proteins

Andy LiWang<sup>a,b,1</sup> and John Orban<sup>c,d,1</sup>

Edited by Adriaan Bax, NIH, Bethesda, MD; received November 6, 2024; accepted February 12, 2025

Metamorphic proteins switch reversibly between two differently folded states under a variety of environmental conditions. Their identification and prediction are gaining attention, but the fundamental physicochemical basis for fold switching remains poorly understood. In this Perspective article, we address this problem by surveying the landscape of well-characterized metamorphic proteins and noting that a significant fraction of them display temperature sensitivity. We then make the case that the dependence on temperature, in particular cold-denaturation effects, is likely to be an underlying property of many metamorphic proteins regardless of their ultimate triggering mechanisms, especially those with a single domain. The argument is supported by rigorous analysis of hydrophobic effects in each well-characterized metamorphic protein pair and a description of how these parameters relate to temperature. The conclusion discusses the relevance of these insights to a better understanding of prediction, evolution, and de novo design strategies for metamorphic proteins.

metamorphic proteins | ambient temperature | protein folding | hydrophobic core | cold denaturation

The traditional one-to-one-to-one relationship between sequence, fold, and function of proteins is currently undergoing significant revision. For example, intrinsically disordered proteins (1) can adopt different folds upon promiscuously binding other proteins, whereas amyloid proteins and prions can change their folds but do so irreversibly (2). Metamorphic proteins, on the other hand, populate two differently folded structures reversibly (3). They are distinct from moonlighting proteins, which have more than one biochemical function but the same fold (4), and morphoeins, which are proteins that adopt different quaternary structures while retaining the same fold (5). Computational analyses have estimated that up to 4% of the folds in the Protein Data Bank are metamorphic (6). But the true extent to which metamorphic proteins are masquerading as single-fold (or monomorphic) proteins, both in the PDB and more generally, remains unknown. Moreover, despite the growing body of data and increasing interest in the prediction and design of alternatively folded states, the essential basis for protein metamorphism has yet to be articulated.

To date, approximately 90 naturally occurring metamorphic proteins have been found and characterized experimentally (6), and new deep-learning methods offer the prospect of identifying more folds that can switch (7–11). Furthermore, it has been shown that metamorphism can be designed into a number of the most commonly occurring protein folds (12). For a protein fold to be metamorphic, it must be in equilibrium with an alternatively folded state. The population of the predominant fold under a specified condition can be shifted

to the alternate fold in the presence of an environmental trigger. In this way, a wide range of environmental conditions (e.g., ligands, redox, pH) can cause fold switching by shifting the equilibrium between metamorphic protein pairs. Nevertheless, how the equilibrium is established in the first place is unclear. Two recent studies on completely unrelated metamorphic proteins, Sa1V90T and KaiB, provide clues in this regard (Fig. 1 A and B). They independently revealed that temperature alone induces reversible transformation from one ordered state to another (13–15). In these cases, it was found that the low-temperature state has a smaller hydrophobic core and is more disordered than the high-temperature state, consistent with a partial cold-denaturation event where hydrophobic forces are known to weaken as temperature decreases (16, 17). This then raises the question of whether differences in the extent of hydrophobic contacts, and the associated temperature sensitivity, are an underlying feature of other metamorphic proteins, regardless of their ultimate triggering mechanisms.

To address this question, a representative list of 26 structurally characterized metamorphic protein pairs (6) were surveyed for differences in the hydrophobic packing effects of their switchable regions, including changes in solvent accessible surface area (SASA). As such, we developed a “Core Score” as a measure of the hydrophobic core of the fold-switching region of a protein that accounts for a) the number of carbon-carbon atom distances  $< 3.8 \text{ \AA}$  and b) SASA (SI Appendix, Table S1). In Fig. 1E we sorted the proteins according to the length of the fold-switching region from left to right and used a vertical dashed line to distinguish proteins with fold-switching regions shorter or longer than 30 residues. Strikingly, most of the metamorphic pairs with switchable regions exceeding 30 amino acids in length had significant differences in their Core Scores, like those seen for KaiB and Sa1V90T. Moreover, where some evidence for temperature sensitivity was either reported or inferred from

Author affiliations: <sup>a</sup>Department of Chemistry and Biochemistry, University of California, Merced, CA 95343; <sup>b</sup>Center for Cellular and Biomolecular Machines, University of California, Merced, CA 95343; <sup>c</sup>William Myron Keck Laboratory for Structural Biology, University of Maryland Institute for Bioscience and Biotechnology Research, Rockville, MD 20850; and <sup>d</sup>Department of Chemistry and Biochemistry, University of Maryland, College Park, MD 20742

Author contributions: A.L. and J.O. designed research; performed research; analyzed data; and wrote the paper.

The authors declare no competing interest.

This article is a PNAS Direct Submission.

Copyright © 2025 the Author(s). Published by PNAS. This article is distributed under Creative Commons Attribution-NonCommercial-NoDerivatives License 4.0 (CC BY-NC-ND).

<sup>1</sup>To whom correspondence may be addressed. Email: aliwang@ucmerced.edu or jorban@umd.edu.

This article contains supporting information online at <https://www.pnas.org/lookup/suppl/doi:10.1073/pnas.2422725122/-DCSupplemental>.

Published March 13, 2025.

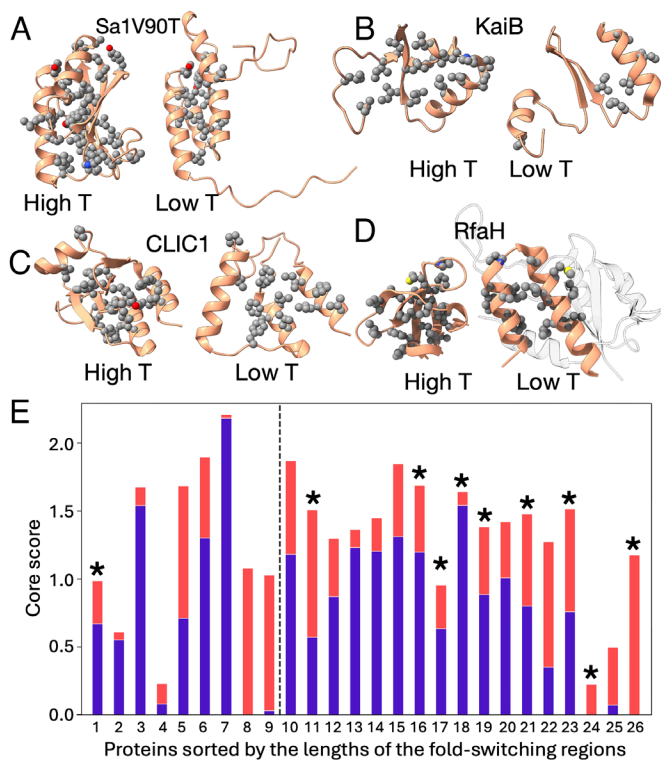


**Fig. 1.** A comparison of hydrophobic cores for representative metamorphic protein pairs. The hydrophobic cores of the fold-switching regions of (A) Sa1V90T, (B) KaiB, (C) CLIC1, and (D) RfaH are shown with the heat- and cold-stable folds on the *Left*- and *Right*-hand sides, respectively. The N-terminal domain of RfaH is rendered as a semitransparent ribbon. The gray, red, and blue spheres represent carbon, oxygen, and nitrogen atoms, respectively. (E) Core scores of 26 metamorphic proteins sorted (*Left to Right*) by the length of the fold-switching region. To the *Left* and *Right* of the dashed vertical line are proteins where the fold-switching region is shorter and longer than 30 residues, respectively. An asterisk is used to identify a protein where there is evidence (direct or indirect) that temperature affects the equilibrium between its two folds with the red and blue colors representing the folds toward which the equilibrium shifts under higher and lower temperatures, respectively. For a protein without an asterisk, the red and blue bars represent the folds toward which the equilibrium is predicted to shift under higher and lower temperatures, respectively. Along the x axis the numbers represent separate proteins as follows: 1 = Sak-Polo, 2 = EphA4, 3 = KSHV, 4 = Mat $\alpha$ 2, 5 = OAS1, 6 = Pima, 7 = caspase, 8 = Piv5, 9 = RAR, 10 = endolysin, 11 = selecasin, 12 = phytochrome, 13 = XRCC1, 14 = fibronectin, 15 = PfPR5, 16 = RfaH, 17 = Sb4, 18 = Mad2, 19 = KaiB, 20 = tachylectin, 21 = Sa1V90T, 22 = IscA, 23 = CLIC1, 24 = XCL1, 25 = Orf9b, 26 = IscU. IscU has a zero-core score at low temperatures because it unfolds. XCL1 has a zero-core score at low temperatures because it is unstable (unfolds) in the cold under the no-salt conditions used for the high temperature structure. Piv5 has a zero-core score at low temperatures because, although folded, it does not have a hydrophobic core under the criteria used for SASA and van der Waals measurements.

biophysical data (*SI Appendix, Table S2*), the low-temperature state possessed fewer hydrophobic contacts than the high-temperature state. Indeed, this trend was supported experimentally for more than half of the proteins with larger switching regions. Together, these observations suggest that a temperature-dependent change in hydrophobicity, in particular partial cold denaturation, plays an important role in establishing the essential equilibrium between metamorphic folds.

The apparent partial cold denaturation effects seen in metamorphic proteins tend to occur at higher temperatures and over a biologically relevant range not found in most monomeric proteins (18). The hallmark features, fewer hydrophobic contacts and buried residues in the putatively

low temperature and more disordered state, may have evolved to provide an adaptive advantage. The clearest example of this so far is for KaiB. KaiB is a single-domain protein where one fold is solely found in KaiB homologs and the other is the common thioredoxin-like fold (19). The low-temperature thioredoxin-like fold is stabilized by binding to the cyanobacterial circadian clock protein, KaiC (the environmental trigger). When KaiC is not receptive to KaiB, homotetramerization helps stabilize the more well-packed high-temperature fold that is unique to KaiB. A prime characteristic of all circadian clocks is that they provide a reliable internal representation of time over a wide range of physiological temperatures through a compensation mechanism. Recent work has suggested that the temperature-dependent equilibrium of the two folds of KaiB is part of the overall mechanism by which the circadian clock of cyanobacteria compensates for changes in ambient temperatures (14). This example raises the intriguing possibility that, especially for ectotherms, the inherent temperature sensitivity of metamorphic proteins is an adaptation to changes in ambient temperature.

However, metamorphic proteins are also present in endothermic organisms, such as mammals, where body temperature is controlled internally and, by itself, is therefore not likely to be the biologically relevant basis for a shape-shifting event. Nonetheless, temperature-dependent partial cold denaturation effects are still observed in such cases, providing an equilibrium between fold switch states. An example of this is the well-characterized human protein lymphotactin (XCL1), which has a temperature/salt dependence that shifts the protein from an all- $\beta$  dimer at 40 °C and no salt to an  $\alpha/\beta$ -monomer at 10 °C and high salt (20). XCL1 unfolds at low temperatures under the zero-salt buffer condition used at 40 °C. While temperature sensitivity plays a critical role in establishing an equilibrium between the low- and high-temperature forms, ligand-binding events probably control fold switching *in vivo*, as evidenced by XCL1's chemokine receptor and glycosaminoglycan binding properties, respectively.

Although XCL1 and Sa1V90T largely transition from one folded state to another within the 0 to 40 °C temperature range, complete interconversion is not a requirement for an effective metamorphic protein. Alternative fold-switched states that are poorly populated can be stabilized to expand functional capacity. For example, the two-domain transcription factor RfaH (21) switches between minimally packed 2- $\alpha$  and well-packed all- $\beta$  C-domain structures with an inferred temperature sensitivity (Fig. 1D). The 2- $\alpha$  state is highly unstable in isolation at 25 °C (22) but is stabilized intramolecularly through association with its N-domain at 15 °C, autoinhibiting the protein in a closed state. In contrast, the all- $\beta$  form is stable on its own at 25 °C, allowing the shift to an open state in which the N- and C-domains separate and interact with stabilizing ligands. Similarly, the N-domain of the chloride ion channel protein, CLIC1 (23), alternates between 3- $\alpha$  and thioredoxin folds depending on the redox condition (Fig. 1C). The 3- $\alpha$  N-domain fold has fewer hydrophobic contacts and is poorly populated at room temperature, but the equilibrium is nonetheless shifted from the well-packed thioredoxin state to 3- $\alpha$  under oxidizing conditions by a stabilizing intramolecular disulfide bridge. The

examples of RfaH and CLIC1 demonstrate the common role of partial cold denaturation in sufficiently populating alternative folds to facilitate switching. They also show that the equilibrium between metamorphic forms can be shifted by intramolecular interactions or intermolecular factors, which act as “environmental” triggers. Additionally, external factors can directly affect either the low- or high-temperature states. These observations also apply to oligomerization, which may be considered a concentration-dependent environmental effect, where either low-temperature states (e.g., CLIC1, sel-ecase) or high-temperature states (e.g., KaiB, XCL1) are involved in the multimerization event.

In the majority of known examples, metamorphic proteins contain a subdomain that undergoes fold interconversion within a larger, mostly invariant structure. This may make partial cold denaturation and temperature effects difficult to measure in some cases because only a small part of the polypeptide chain is participating in the structural transitions. The data in Fig. 1E further amplify this point. Metamorphic proteins with fewer than 30 amino acids involved in the fold switch have smaller differences in hydrophobic packing effects between the two states in some cases, suggesting that temperature sensitivity may be attenuated. In contrast, metamorphs involving greater than 30 residues generally display more consistent differences in their hydrophobic packing tendencies. It is perhaps then not a coincidence that two of the examples where the relative contributions of the switching regions are among the largest known, Sa1V90T and KaiB, also happen to have the most clearly described experimental support for cold denaturation effects. In both these instances, at least 50% of the polypeptide chain contributes to the fold interconversion, presumably making temperature sensitivity effects more readily detectable.

Even though the phenomenon of cold denaturation is well known and is predicted by the Gibbs–Helmholtz equation, the exact mechanisms responsible are still being actively debated. The generally held view is that introducing a nonpolar solute into bulk water induces the formation of hydrating clathrate structures, which reduces the overall entropy. However, as the temperature of the system decreases, the clathrate structures become more stable (more enthalpically favorable) and the entropic penalty is minimized because the water molecules are already more ordered (16, 17, 24). Thus, as water cools, it solvates hydrophobic surfaces more readily, thereby weakening the nonpolar interactions that help to stabilize folded states and contributing to at least partial unfolding (25). More recently, molecular dynamics

simulations have suggested that the primary driving force for cold denaturation is not due so much to attenuation of hydrophobic effects but largely because of more favorable solvent-bridged hydrogen bonds between polar residues as the temperature is lowered (26). Regardless of the exact physicochemical mechanism, there are fewer hydrophobic contacts and buried residues in partially cold-denatured states, and these features parallel the principal metrics in our analysis of metamorphic protein pairs.

In summary, we postulate that the fold-switching free-energy landscapes of metamorphic proteins are especially sensitive to changes in ambient temperature (i.e., in the 0 to 40 °C range) even though most shape-shifting events have additional environmental cues. We recognize that the conformational states of monomeric proteins can also be temperature responsive over this range. However, we propose that ambient temperature-dependent effects are more significant in metamorphic protein pairs due to the generally notable difference in their hydrophobic cores. The idea that the fold-switching equilibria of many metamorphic proteins are inherently temperature-dependent has implications for understanding the evolutionary pressures under which this special class of proteins provides an adaptive advantage. With KaiB as the clearest example so far, we think that for ectotherms in particular, metamorphic proteins may have evolved so that these organisms could readily adapt to changes in ambient temperature. How this mechanism might have evolved in endotherms is an open and intriguing question that may lead to new insights into the evolution of protein folds. Moreover, despite recent progress, significant challenges remain in the prediction and design of metamorphic proteins. To address these challenges, it appears that the fundamental effects of temperature on metamorphic states will need to be critically considered. This will be especially true as physics-based computational approaches such as molecular dynamics become more efficient, enabling their use in conjunction with deep-learning methods to map the energy landscapes of transitions between metamorphic states.

**Data, Materials, and Software Availability.** All study data are included in the article and/or *SI Appendix*.

**ACKNOWLEDGMENTS.** This work was supported by US NIH grants R35GM144110 (to A.L.) and R01GM062154 (to J.O.), US Army grant W911NF-23-1-0248 (to A.L.), and NSF-CREST: Center for Cellular and Biomolecular Machines at the University of California, Merced (NSF-HRD-1547848). The University of Maryland NMR Facility at the Institute for Bioscience & Biotechnology Research is additionally supported by the National Institute of Standards and Technology and a grant from the William Myron Keck Foundation.

1. A. S. Holehouse, B. B. Kragelund, The molecular basis for cellular function of intrinsically disordered protein regions. *Nat. Rev. Mol. Cell Biol.* **25**, 187–211 (2024).
2. D. Willbold, B. Strodel, G. F. Schröder, W. Hoyer, H. Heise, Amyloid-type protein aggregation and prion-like properties of amyloids. *Chem. Rev.* **121**, 8285–8307 (2021).
3. A. G. Murzin, Biochemistry metamorphic proteins. *Science* **320**, 1725–1726 (2008).
4. C. J. Jeffery, Moonlighting proteins. *Trends Biochem. Sci.* **24**, 8–11 (1999).
5. E. K. Jaffe, Morpheins—a new structural paradigm for allosteric regulation. *Trends Biochem. Sci.* **30**, 490–497 (2005).
6. L. L. Porter, L. L. Looger, Extant fold-switching proteins are widespread. *Proc. Natl. Acad. Sci. U.S.A.* **115**, 5968–5973 (2018).
7. H. K. Wayment-Steele *et al.*, Predicting multiple conformations via sequence clustering and AlphaFold2. *Nature* **625**, 832–839 (2024).
8. N. Chen, M. Das, A. LiWang, L.-P. Wang, Sequence-based prediction of metamorphic behavior in proteins. *Biophys. J.* **119**, 1380–1390 (2020).
9. S. Mishra, L. L. Looger, L. L. Porter, Inaccurate secondary structure predictions often indicate protein fold switching. *Protein Sci.* **28**, 1487–1493 (2019).
10. L. L. Porter, Fluid protein fold space and its implications. *Bioessays* **45**, e2300057 (2023).
11. L. L. Porter, I. Artsimovitch, C. A. Ramirez-Sarmiento, Metamorphic proteins and how to find them. *Curr. Opin. Struct. Biol.* **86**, 102807 (2024).
12. B. Ruan *et al.*, Design and characterization of a protein fold switching network. *Nat. Commun.* **14**, 431 (2023).
13. T. L. Solomon *et al.*, Reversible switching between two common protein folds in a designed system using only temperature. *Proc. Natl. Acad. Sci. U.S.A.* **120**, e2215418120 (2023).
14. N. Zhang *et al.*, Temperature-dependent fold-switching mechanism of the circadian clock protein KaiB. *Proc. Natl. Acad. Sci. U.S.A.* **121**, e2412327121 (2024).

15. H. K. Wayment-Steele *et al.*, The conformational landscape of fold-switcher KaiB is tuned to the circadian rhythm timescale. *Proc. Natl. Acad. Sci. U.S.A.* **121**, e2412293121 (2024).
16. E. van Dijk, A. Hoogeveen, S. Abeln, The hydrophobic temperature dependence of amino acids directly calculated from protein structures. *PLoS Comput. Biol.* **11**, e1004277 (2015).
17. C. L. Dias, T. Ala-Nissila, M. Karttunen, I. Vattulainen, M. Grant, Microscopic mechanism for cold denaturation. *Phys. Rev. Lett.* **100**, 118101 (2008).
18. J. Soto, S. L. Moro, M. J. Cocco, Dynamics and thermal stability of the bypass polymerase, DinB homolog (Dbh). *Front. Mol. Biosci.* **11**, 1364068 (2024), 10.3389/fmolb.2024.1364068.
19. Y.-G. Chang *et al.*, A protein fold switch joins the circadian oscillator to clock output in cyanobacteria. *Science* **349**, 324–328 (2015).
20. R. L. Tuinstra *et al.*, Interconversion between two unrelated protein folds in the lymphotactin native state. *Proc. Natl. Acad. Sci. U.S.A.* **105**, 5057–5062 (2008).
21. B. M. Burmann *et al.*, An  $\alpha$  helix to  $\beta$  barrel domain switch transforms the transcription factor RfaH into a translation factor. *Cell* **150**, 291–303 (2012).
22. P. K. Zuber *et al.*, Structural and thermodynamic analyses of the  $\beta$ -to- $\alpha$  transformation in RfaH reveal principles of fold-switching proteins. *eLife* **11**, e76630 (2022), 10.7554/eLife.76630.
23. D. R. Littler *et al.*, The intracellular chloride ion channel protein CLIC1 undergoes a redox-controlled structural transition. *J. Biol. Chem.* **279**, 9298–9305 (2004).
24. C. L. Dias *et al.*, The hydrophobic effect and its role in cold denaturation. *Cryobiology* **60**, 91–99 (2010).
25. P. L. Privalov, Cold denaturation of protein. *Crit. Rev. Biochem. Mol. Biol.* **25**, 281–306 (1990).
26. S. R. Durell, A. Ben-Naim, Temperature dependence of hydrophobic and hydrophilic forces and interactions. *J. Phys. Chem. B* **125**, 13137–13146 (2021).

**Table S1. Core Scores for a Representative Set of Metamorphic Proteins<sup>a</sup>.**

Protein	Core Score <sup>b</sup>		Chain: Region
	Lower temp	Higher temp	
Sak-Polo	0.67 (0.67, 0.00) 0.99 (0.50, 0.17)		1MBY.A: 908-919 2N19.A: 953-964
EphA4	0.55 (0.38, 0.08) 0.61 (0.46, 0.08)		4M4R.A: 154-166 4W50.A: 154-166
KSHV	1.54 (0.90, 0.25) 1.68 (0.75, 0.30)		3NJQ.B: 11-30 2PBK.A: 11-30
Mata2	0.08 (0.08, 0.00) 0.23 (0.23, 0.00)		1MNM.D: 116-128 1MNM.C: 116-128
OAS1	0.71 (0.71, 0.00) 1.69 (0.86, 0.29)		4RWQ.A: 61-74 4RWN.A: 61-74
PimA	1.30 (0.94, 0.18) 1.90 (1.47, 0.24)		4N9W.A: 118-134 4NC9.C: 118-134
caspase	2.18 (1.43, 0.33) 2.21 (1.67, 0.29)		2WDP.A: 119-139 3OD5.A: 119-139
Piv5	0.00 (0.00, 0.00) 1.08 (1.05, 0.05)		1SVF.A: 147-168 4WSG.C: 147-168
Retinoic acid receptor	0.03 (0.03, 0.00) 1.03 (0.58, 0.17)		3KMZ.A: 393-421 3KMR.A: 393-421
endolysin	1.18 (0.87, 0.16) 1.87 (0.97, 0.32)		1XJU.A: 39-69 1XJT.A: 39-69
selecase	0.57 (0.57, 0.00) 1.51 (1.28, 0.16)		4QHH.A: 78-109 4QHF.A: 78-109
phytochrome	0.87 (0.63, 0.12) 1.30 (1.15, 0.12)		4O01.A: 446-478 4O0P.A: 446-478
XRCC1	1.23 (0.84, 0.18) 1.36 (0.87, 0.21)		AF3: 1-39 3IQC.A: 1-39
fibronectin	1.20 (0.98, 0.14) 1.45 (1.05, 0.20)		3EJH.A: 516-559 3M7P.A: 516-559
PfPRS	1.31 (1.04, 0.16) 1.85 (1.08, 0.30)		4YDQ.A: 318-367 4TWA.A: 318-367
RfaH	1.20 (1.16, 0.06) 1.69 (1.36, 0.20)		8PIB.P: 113-162 8PHK.P: 113-162
Sb4	0.63 (0.39, 0.10) 0.96 (0.65, 0.14)		9A1D <sup>pdbev</sup> .A: 1-21, 57-87 7MP7.A: 1-21, 57-87
Mad2	1.54 (1.42, 0.12) 1.64 (1.34, 0.19)		2V64.E: 1-16, 164-204 2V64.A,B: 1-16, 164-204
KaiB	0.89 (0.47, 0.15) 1.38 (1.05, 0.18)		5JWO.B: 47-108 1VGL.B: 47-108
tachylectin	1.01 (0.81, 0.12) 1.42 (1.10, 0.18)		3KIF.A: 1-72 3KIH.A: 26-97
Sa1V90T	0.80 (0.53, 0.12) 1.48 (0.93, 0.23)		9A20 <sup>pdbev</sup> .A: 1-15, 34-95 8E6Y.A: 1-15, 34-95
IscA	0.35 (0.35, 0.00) 1.27 (0.99, 0.16)		1X0G.D: 26-110 1x0G.A: 26-110
CLIC1	0.76 (0.57, 0.10) 1.52 (0.78, 0.26)		1RK4.A: 1-89 1K0M.A: 1-89
XCL1	0.00 (0.00, 0.00) 0.23 (0.18, 0.01)		Unstable under zero salt. 2JP1.A: 54-70
Orf9b	0.07 (0.05, 0.01) 0.50 (0.43, 0.05)		7KDT.B: 1-97 6Z4U.A: 1-97
IscU	0.00 (0.00, 0.00) 1.18 (0.42, 0.22)		Denatured at low temperature. 1R9P.A: 1-128

<sup>a</sup>The fraction of residues with  $\leq 10\%$  solvent accessible surface area (SASA) was calculated utilizing Pymol (Schrodinger, LLC) as follows: after the fold switch region was specified, the compute > surface area > relative solvent accessibility command string was executed. From the output, the number of residues with SASA  $\leq 10\%$  was determined as a fraction of the total number of residues in the polypeptide chain. The number of van der Waals (vdW) contacts per fold-switching residue was calculated in ChimeraX (doi 10.1002/pro.4792) using the “contacts” command. For example, to determine the vdW value for the KaiB structure, 5JWO.B, where the fold-switching region encompasses residues 47 – 108 (62 residues), we executed the following command:

“contacts /B:47-108@C\* restrict /B@C\* distance 3.8 reveal true name vdW”

Accordingly, there are  $29/62 = 0.47$  vdW contacts/residue. Residues having no electron density were presumed to be disordered but were nevertheless included in the total amino acid count.

The Core Score was calculated by accounting for (a) vdW contacts/residue and (b) SASA as follows: Core Score =  $\sqrt{a^2 + (5*b)^2}$ . SASA values were multiplied by 5 so that they are weighted more evenly with vdW values (in analogy with NMR chemical shift perturbation calculations).

This representative set of metamorphic proteins was obtained from a paper by Porter and Looger (doi 10.1073/pnas.1800168115).

Both the vdW and SASA calculations were in the context of the full monomeric structure, including interdomain effects. Intermolecular interactions were not included in the Core Score because we assume that fold switching occurs in the monomeric form.

<sup>b</sup>Core scores for each fold. In parentheses are the vdW contacts/residue and SASA values, in that order, for each fold.

**Table S2:** Experimental support for temperature-dependent metamorphic states

Protein	PDB/ PDBDev code	Lower/Higher Temperature State	Experimental evidence	Reference
CLIC1	1RK4.A	Lower (inferred)	Addition of hydrogen peroxide at room temperature leads to formation of a dimer by size exclusion chromatography (SEC), which is mediated by self-association through the 3- $\alpha$ N-domain. This indicates that a small equilibrium population of the putatively low temperature 3- $\alpha$ N-domain fold must be present prior to the addition of oxidizing agent, and that the 3- $\alpha$ state is stabilized by an intramolecular disulfide.	Littler <i>et al.</i> (2004) <i>J. Biol. Chem.</i> 279, 9298-9305.
	1K0M.A	Higher (inferred)	CLIC1 is monomeric at room temperature by SEC in the absence of oxidizing agents. This indicates that the major population for its N-domain in the higher temperature state is the thioredoxin fold.	
IscU	-	Lower (known)	IscU is significantly unfolded at low temperature.	Bothe <i>et al.</i> (2015) <i>Biophys. J.</i> 109, 1019-1025.
	1R9P.A	Higher (known)	IscU adopts a stable fold at room temperature as determined by NMR spectroscopy.	
KaiB	5JWO.B	Lower (known)	NMR data indicate that the equilibrium shifts toward the thioredoxin fold at lower temperatures.	Zhang <i>et al.</i> (2024) <i>PNAS</i> 121, e2412327121
	1VGL.A	Higher (known)	NMR spectra indicate that the equilibrium increasingly favors the unique fold of KaiB at higher temperatures.	
Mad2	2V64.E	Lower (known)	Mad2 is stable in the open form at 4 °C, as determined by NMR.	Luo <i>et al.</i> (2004) <i>Nat. Str. Mol. Biol.</i> 11, 338-245.
	2V64.A	Higher (known)	Mad2 is stable in the closed form at 30 °C, as determined by NMR.	
RfaH	8PIB.B	Lower (inferred)	The 2- $\alpha$ C-domain is unstable in isolation at 25 °C. In full-length RfaH, the 2- $\alpha$ C-domain is stabilized by interactions with the N-domain at 15 °C, as determined by NMR.	Burmam <i>et al.</i> (2012) <i>Cell</i> 150, 291-303.
	8PHK.P	Higher (inferred)	The all- $\beta$ C-domain is stable at 25 °C, as determined by NMR.	
Sa1V90T	00000132	Lower (known)	Sa1V90T has a 3- $\alpha$ fold at 5 °C, as determined by NMR spectroscopy.	Solomon <i>et al.</i> (2023) <i>PNAS</i> 120, e2215418120.

	8E6Y	Higher (known)	Sa1V90T has an $\alpha\beta$ -plait fold at 30 °C, as determined by NMR spectroscopy.	
Sak-Polo	1MBY.A	Lower (inferred)	Domain-swapped dimer with a C-terminal $\beta$ -strand, determined by X-ray crystallography. However, this form is weakly populated in solution at 20 °C by NMR. Arquint <i>et al.</i> suggest that either X-ray conditions shift the equilibrium to this state or that the dimer crystallizes preferentially.	Leung <i>et al.</i> (2002) <i>Nat. Str. Biol.</i> 9, 719-724.
	2N19.A	Higher (inferred)	Monomer in solution at 20 °C with a C-terminal $\alpha$ -helix by NMR spectroscopy. An X-ray structure of a complex with a cognate ligand and mutational studies support the monomer as the known biologically relevant form.	Arquint <i>et al.</i> (2015) <i>eLife</i> 4, e07888.
Sb4	00000085	Lower (known)	The $\beta$ -grasp fold of Sb4 is more populated below 25 °C as determined by NMR spectroscopy.	Ruan <i>et al.</i> (2023) <i>Nat. Commun.</i> 14, 431.
	7MP7	Higher (known)	The $\alpha\beta$ -plait fold of Sb4 is more populated at 30 °C as observed by NMR spectroscopy.	
Selecase	4QHH	Lower (inferred)	The putatively low temperature form is only seen in the tetramer state, which is weakly populated at room temperature by SEC and SDS-PAGE crosslinking experiments. Also, tetramer crystals grow best below ambient temperature.	Lopez-Pelegrin <i>et al.</i> (2014) <i>Angew. Chem. Int. Ed.</i> 53, 10624-10630.
	4QHF	Higher (inferred)	The putatively high temperature form is seen in monomer and dimer states, which are well populated at room temperature by SEC and SDS-PAGE crosslinking experiments. Monomer and dimer crystals grow best at ambient temperature. Also, solvation free energy of folding values, calculated using PISA software on the X-ray structures of the monomer subunits, indicate that 4QHF is more stable than 4QHH.	
XCL1	1J8I	Lower (known)	XCL1 adopts a monomeric $\alpha/\beta$ -sandwich fold at 10 °C with 200 mM NaCl, as determined by NMR spectroscopy. We assume that the protein is not well folded in the absence of NaCl.	Tuinstra <i>et al.</i> (2008) <i>PNAS</i> 105, 5057-5062.
	2JP1	Higher (known)	At 40 °C and 0 mM NaCl, XCL1 forms a dimeric $\beta$ -sandwich fold, as determined by NMR.	